Thermal convection in subsurface oceans with variable thickness: Application to Enceladus.

Jeffrey Nederend, Marc Rovira-Navarro and Tiago Pestana

Faculty of Aerospace Engineering, Delft University of Technology, Kluyverweg 1/2, 2629 HS, Delft, The Netherlands

PRESENTED AT:

AGU FALL MEETING
Online Everywhere | 1–17 December 2020

1. A UNIQUE SUBSURFACE OCEAN

Saturn's icy moon **Enceladus** harbours a **global subsurface ocean**. **Tidal heating** in the rocky mantle (Choblet et al., 2017 (https://www.nature.com/articles/s41550-017-0289-8); Liao, Nimmo & Neufeld, 2020 (https://agupubs.onlinelibrary.wiley.com/doi/abs/10.1029/2019JE006209)) **drives ocean currents** and promotes the exchange of energy and mass between the core and ice shell. Understanding this process is key to comprehend the moon's **complex dynamics** and assess its potential **habitability**.

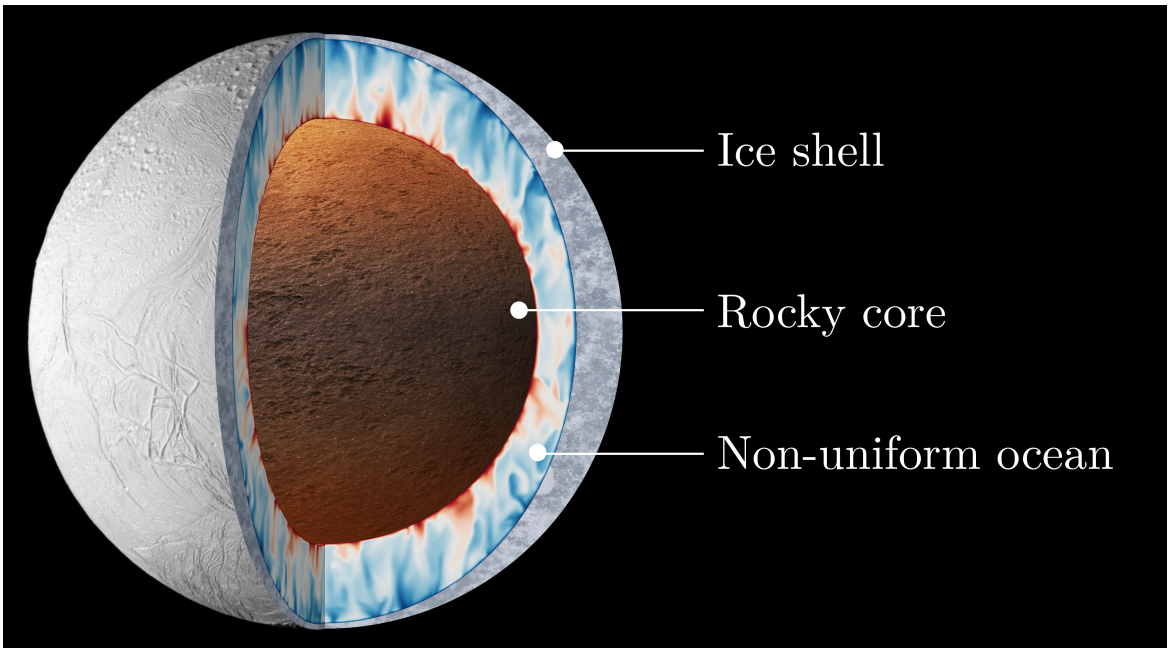

Figure 1. Artistic impression of Enceladus' interior comprising three distinct layers. The heterogeneous ocean floor heat flux is visualised on the core, which lies beneath an ocean and ice shell of variable thicknesses.

Previous models of Enceladus ocean have considered an **ocean of constant thickness** and **uniform heating** at the core-ocean interface (Soderlund, 2019 (https://agupubs.onlinelibrary.wiley.com/doi/full/10.1029/2018GL081880)), even though Cassini observations and current models suggests that this is not the case. Tidal dissipation models of the core suggest that **tidal heat is enhanced in polar regions** (Choblet et al., 2017 (https://www.nature.com/articles/s41550-017-0289-8); Liao, Nimmo & Neufeld, 2020 (https://agupubs.onlinelibrary.wiley.com/doi/abs/10.1029/2019JE006209)). Further, the subsurface **ocean** of Enceladus significantly **varies in thickness**. At the South Pole, strong heat signatures are associated with a thin ice shell (~5-10 km) and thick ocean (~40-50 km) (Čadek et al., 2019 (https://www.sciencedirect.com/science/article/pii/S0019103518303762); Hemingway & Mittal, 2019 (https://www.sciencedirect.com/science/article/pii/S0019103518306882)).

In this study, we analyse the impact that this **non-uniform shape** has on **thermal convection**.

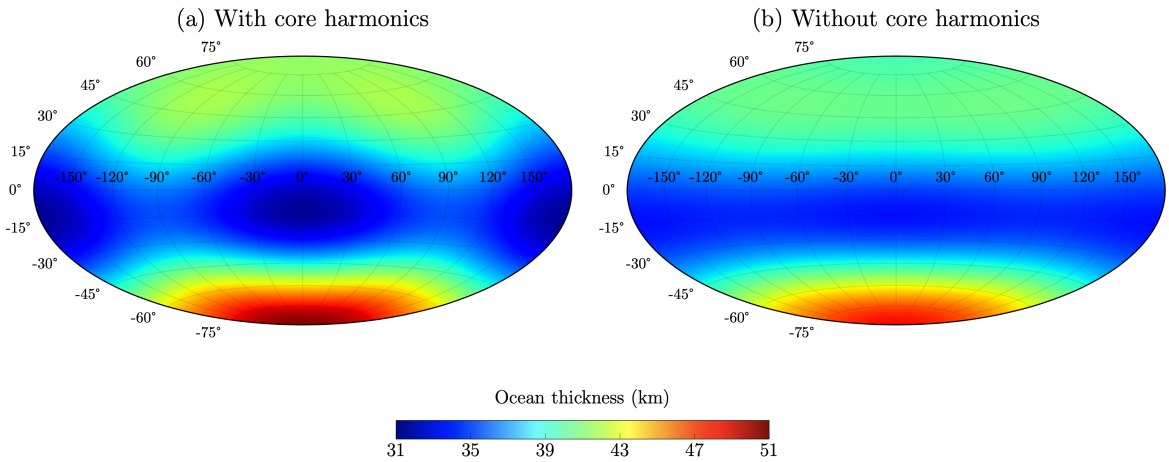

Figure 2. Enceladus' ocean thickness visualised in a hammer projection. Results used from Čadek et al. (2019) (http://www.sciencedirect.com/science/article/pii/S0019103518303762) for spherical harmonic expansion coefficients C20,C22,C30, with mean radii of 194 and 232.1 km for the core-ocean and ocean-ice interfaces respectively.

2. SIMULATING THERMAL CONVECTION

We **model** the subsurface ocean of Enceladus using **3D direct numerical simulations** of **rotating spherical shells**. **Two configurations** are considered: one where the **ocean thickness is constant** and another where the **ocean thickness varies with latitude** and is thicker at the poles than at the equator. Thermal convection is induced by imposing a temperature difference between the boundaries (bottom is hot, top is cold), which are also impenetrable and satisfy the no-slip condition.

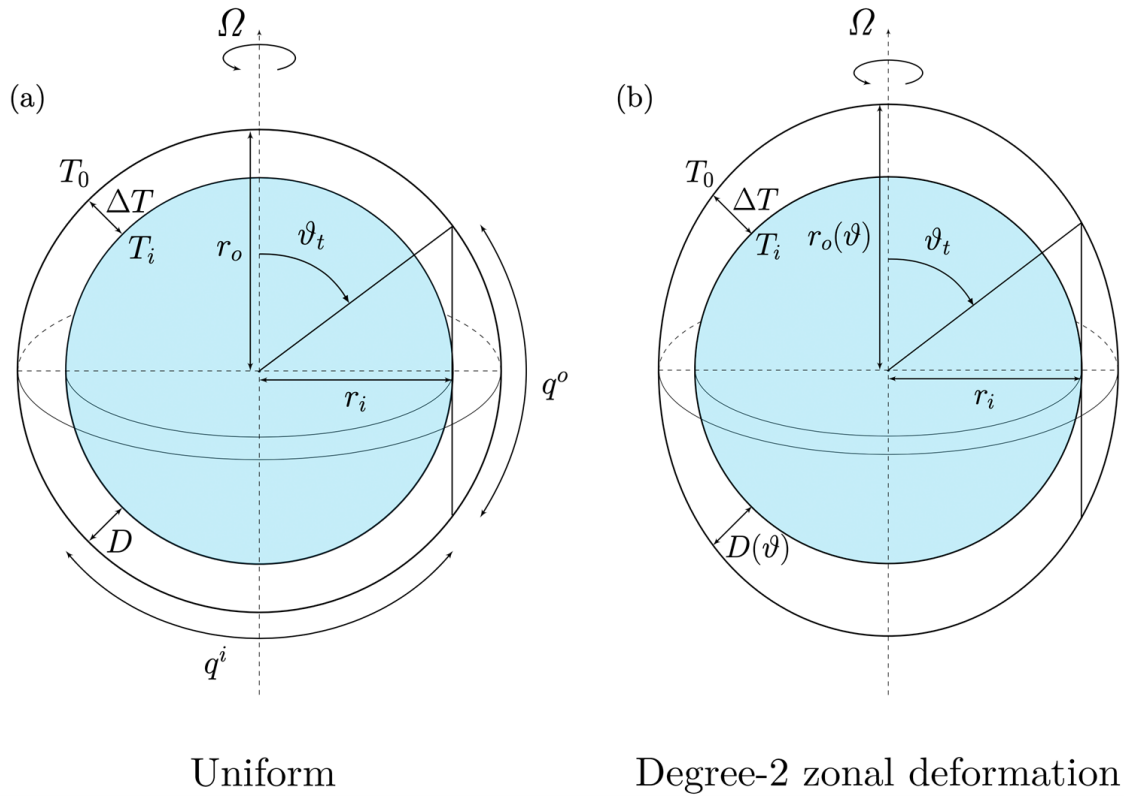

Figure 3. Sketch of the two ocean geometries considered in this study: a constant (a) and variable (b) thickness ocean. A temperature difference is imposed between the two shells. The tangent cylinder is indicated by the angle θ_t and the intersection of the inner sphere equator. We will show the heat flux distribution among the poles and equator using the tangent cylinder demarcation.

In total we conducted 16 simulations and all runs were performed using the **spectral element solver** Nek5000 (https://nek5000.mcs.anl.gov/). To obtain the non-uniform geometry, we added a spherical harmonic perturbation function to the uniform geometry such that the mean ocean thickness D is identical in both geometries.

We solve the non-dimensional equations of motion:

$$\nabla \cdot \boldsymbol{u} = 0,$$

$$\frac{\partial \boldsymbol{u}}{\partial t} + \boldsymbol{u} \cdot \nabla \boldsymbol{u} + 2\,\hat{\boldsymbol{e}}_z \times \boldsymbol{u} = -\nabla P + Ek\nabla^2 \boldsymbol{u} + Ra^* \frac{\boldsymbol{r}}{r_o} T,$$

$$\frac{\partial T}{\partial t} + \boldsymbol{u} \cdot \nabla T = \frac{Ek}{Pr} \nabla^2 T.$$

Here $\boldsymbol{u}, P, \boldsymbol{r}, r_o, T$ are the velocity, reduced pressure, position vector, ice shell base radius and temperature respectively. The non-dimensional modified Rayleigh, traditional Rayleigh, Ekman and Prandtl numbers are given by

$$Ra^* = \frac{RaEk^2}{Pr}, \quad Ra = \frac{\alpha_T g_0 \Delta T D^3}{\nu\kappa}, \quad Ek = \frac{\nu}{\Omega D^2}, \quad Pr = \frac{\nu}{\kappa}.$$

Due to limited computational power, simulations at the Rayleigh and Ekman numbers of Enceladus are not possible. To study the difference in heat transfer behaviour between an ocean of constant and variable thickness, we **simulate thermal convection with varying strength in thermal forcing** that span **two different flow regimes**, i.e., weakly non-linear (strongly influenced by Coriolis) and transitional (weakly influenced by Coriolis) for a constant Ekman number of 3×10^{-4} (see Figure 4) (Gastine, Wicht & Aubert, 2016 (https://www.cambridge.org/core/journals/journal-of-fluid-mechanics/article/scaling- regimes-in-spherical-shell-rotating-convection/1FA9F85A37787E873CE83544FB476D02)).

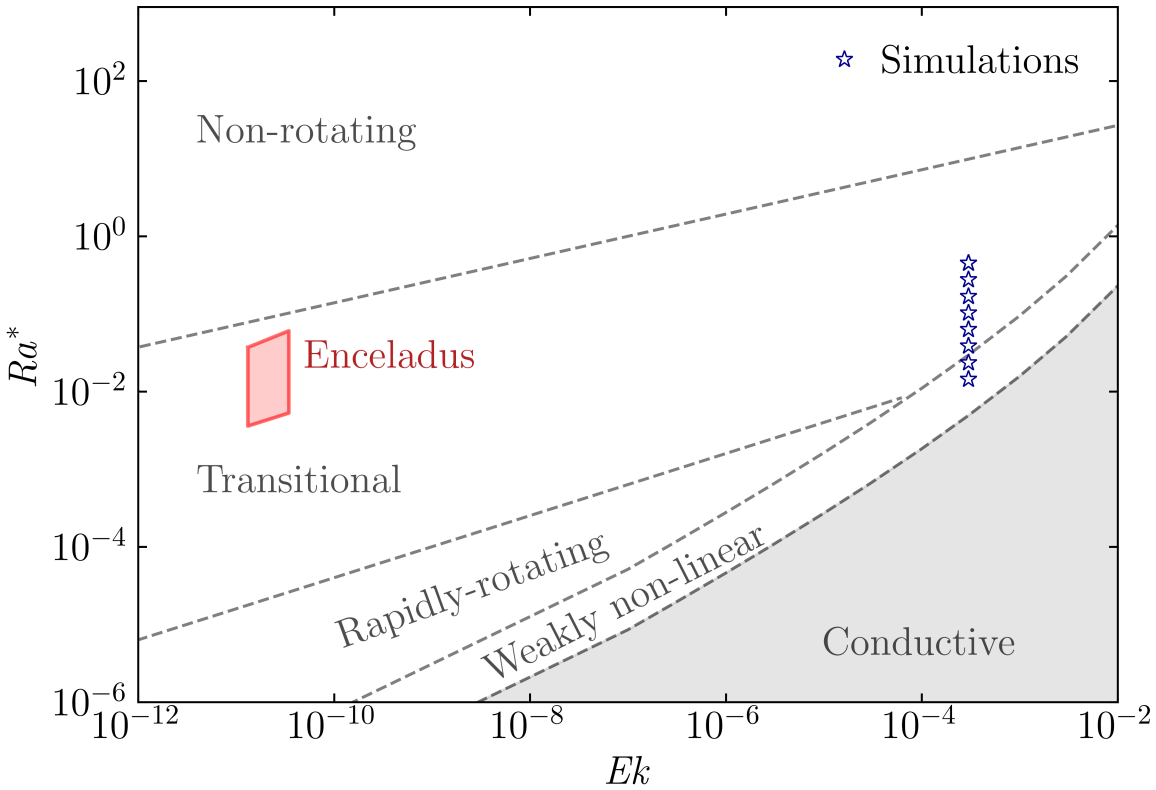

Figure 4. Simulation parameter space with estimated range for Enceladus. Simulation cases are annotated with blue star symbols. Regime boundaries follow from Gastine, Wicht & Aubert (2016) (https://www.cambridge.org/core/journals/journal-of-fluid-mechanics/article/scaling- regimes-in-spherical-shell-rotating-convection/1FA9F85A37787E873CE83544FB476D02).

3. HEAT TRANSPORT BEHAVIOUR

Overall, we find that the **flow morphology is similar** in both cases. **Convection onsets at the equator** with a stagnant polar ocean and gradually starts to shift towards higher latitudes. As thermal forcing increases, **heat transport** at the **poles** becomes **more efficient than at the equator**. One notable difference is that, for the non-uniform model, convection onsets at the poles for a lower global Ra due to the increased local Rayleigh number.

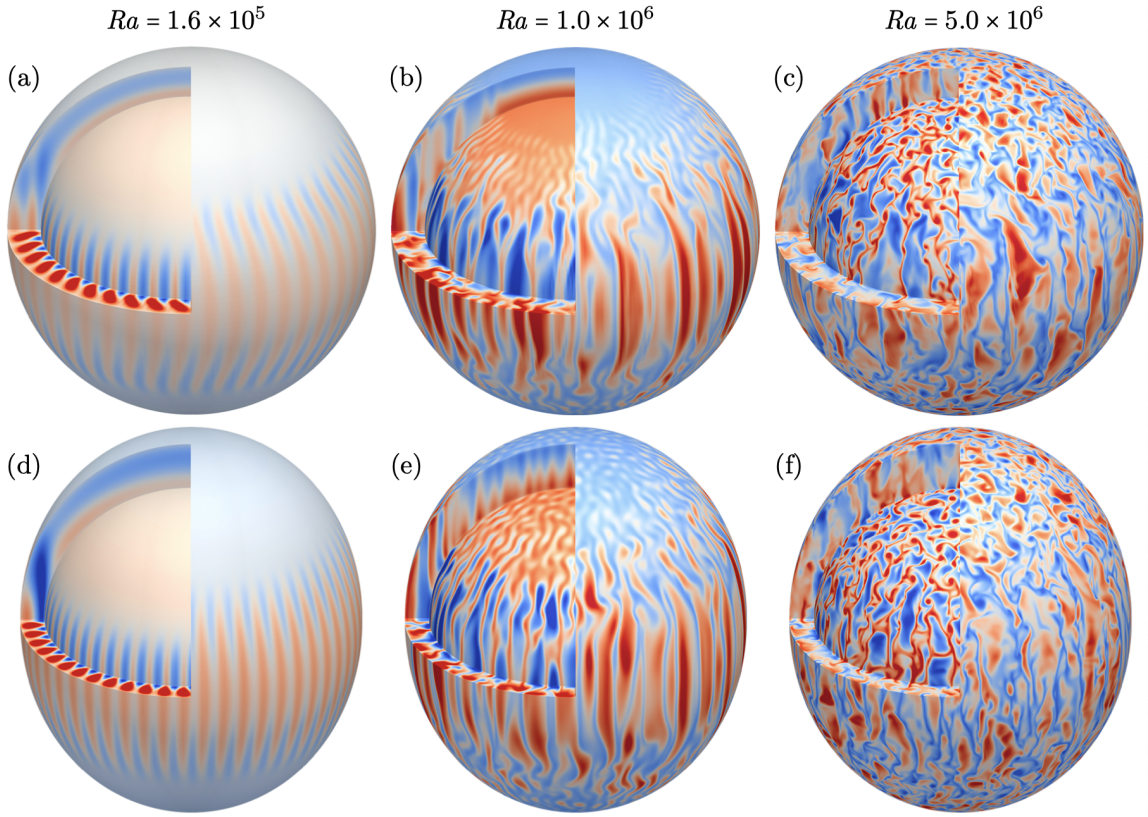

Figure 5. Snapshots of temperature fluctuation fields for three cases representing the lowest, middle and highest Rayleigh number cases simulated. Red/Blue indicate higher/lower temperature than the temporal average for a radial level in the domain.

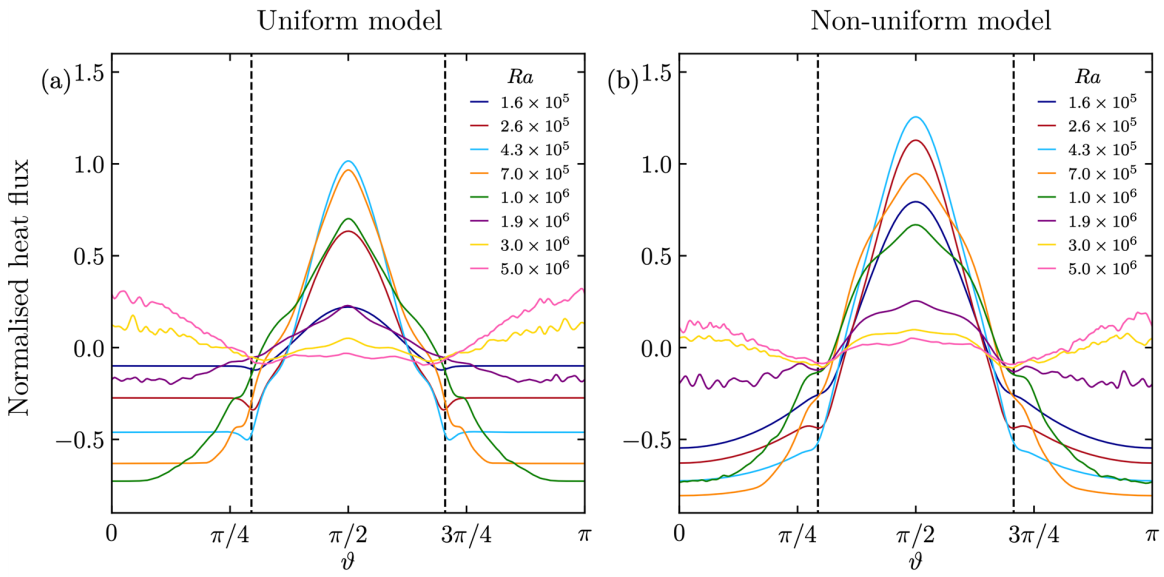

Figure 6. Time and zonally averaged normalised heat flux profiles for the uniform (a) and non-uniform (b) spherical shell geometries. The tangent cylinder angle, unique to each geometry, is shown by the dashed black vertical lines.

Depending on whether heat transport is more efficient at the equator or at the pole, **two regimes** can be identified: **equatorial** or **polar cooling**. The onset of convection is associated with dominant heat transport at the equator (i.e., Equatorial cooling) that initially decreases with increasing Ra in both cases (see Figure 6). Onset of convection at the poles lead to a transition where ultimately the polar heat transport becomes dominant (i.e., Polar
cooling). While this transition is evident for both the oceans of constant and variable thickness, **polar cooling is less efficient** in the latter case.

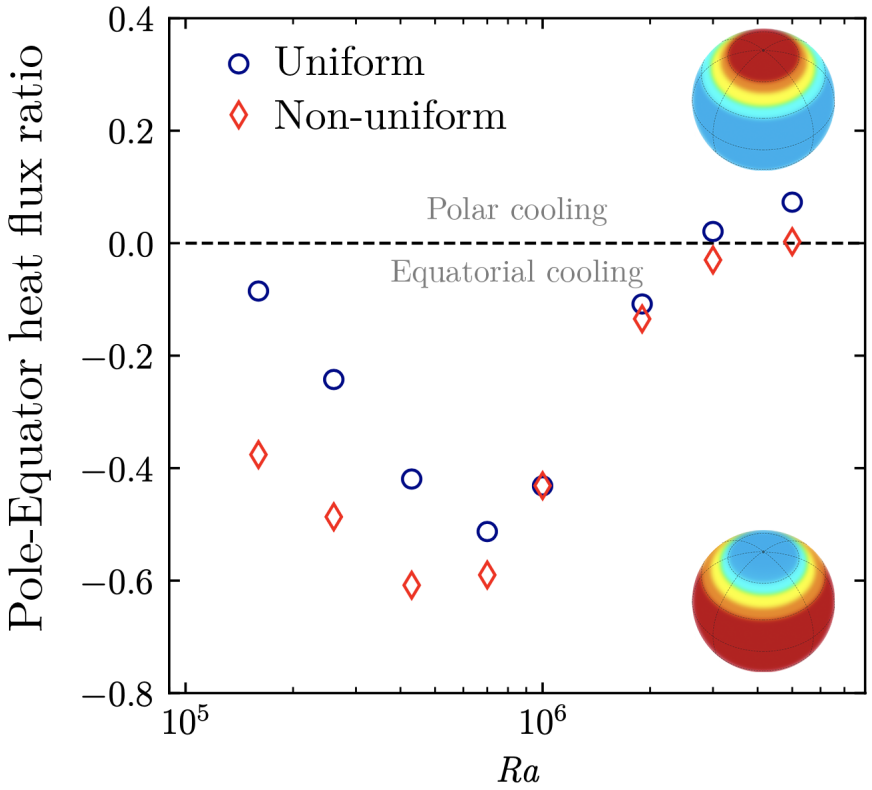

Figure 7. Relative contributions of outer boundary heat flux between regions outside and inside the tangent cylinder demarcating the polar and equatorial regions. Colour and symbol denote the model geometries as indicated in the legend and the horizontal dashed black line in (a) divides the equatorial (negative, outside cylinder) and polar (positive, inside tangent cylinder) dominated heat flux regions. Impression of polar and equatorial cooling are shown on the right to indicate the definitions of both cooling patterns.

The **global heat transport efficiency**, as characterised by the Nusselt number (Nu), **behaves similarly for both geometries** with increasing thermal forcing (Ra). This indicates that **heat transport scaling laws** of **uniform geometries** (e.g., Gastine, Wicht & Aubert, 2016 (https://www.cambridge.org/core/journals/journal-of-fluid-mechanics/article/scaling- regimes-in-spherical-shell-rotating-convection/1FA9F85A37787E873CE83544FB476D02)) can be **applied to** estimate the efficiency of heat transport in the **non-uniform ocean geometry** considered in this study.

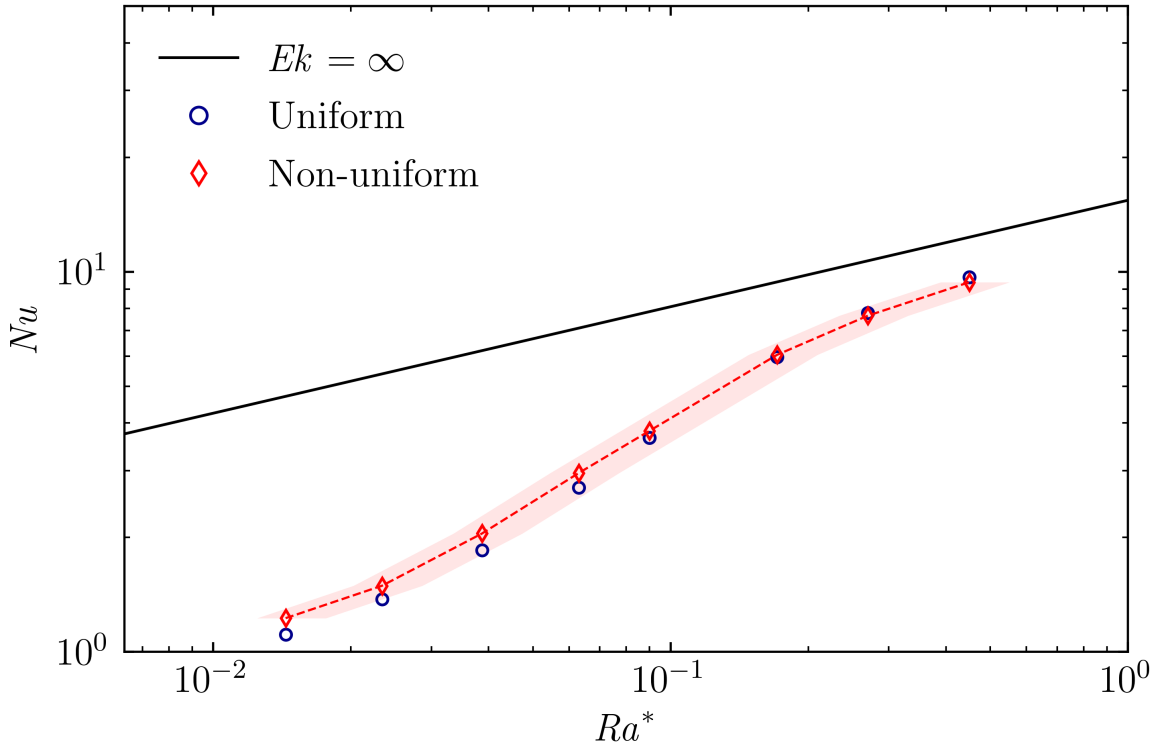

Figure 8. Relation Nusselt and modified Rayleigh numbers for the two shell geometries denoted by colour and shape. The solid black line is the effective Nusselt number upper boundary for a given (modified) Rayleigh number found in non-rotating convection, given by $Nu = 0.164Ra^{0.280}$. The shaded red area demarcates the range of effective modified Rayleigh numbers locally inside the ocean introduced by the variable ocean thickness.

4. CONCLUSIONS

- We compared thermal convection for an ocean of constant thickness with an ocean with a degree-two thickness variation and find that the **impact on thermal convection is minor**.
- At the **poles**, **convection onsets at lower** Ra for **non-uniform** geometry due to a higher local Rayleigh number.
- **Heat transport** at the ice shell base is **stronger at the equator** and **weaker at the poles** for the ocean with **variable thickness**.

5. FUTURE WORK

Due to the weakened polar heat transport, our results suggest that **stronger additional heat transport is required to be consistent** with current predictions of Enceladus' heat profile.

Continuing this project, we will focus on:

- Incorporating **heterogeneous heat flux boundaries** with low degree, high amplitude zonal profile (Choblet et al., 2017 (https://www.nature.com/articles/s41550-017-0289-8); Liao, Nimmo & Neufeld, 2020 (https://agupubs.onlinelibrary.wiley.com/doi/abs/10.1029/2019JE006209))
- Expanding model to simulate **mechanical forces** (i.e., tides, precession and libration) in addition to thermal convection
- Expanding the parameter space with **smaller Ekman numbers** to explore a **rapidly rotating regime** (Gastine, Wicht & Aubert, 2016 (https://www.cambridge.org/core/journals/journal-of-fluid-mechanics/article/scaling-regimes-in-spherical-shell-rotating-convection/1FA9F85A37787E873CE83544FB476D02)).

AUTHOR INFORMATION

Email address for correspondence: Jeffreynederend@hotmail.com

Jeffrey Nederend:

Google Scholar (https://scholar.google.com/citations?user=lsEAONQAAAAJ&hl=en&oi=ao) - LinkedIn (https://www.linkedin.com/in/jeffreynederend/)

Marc Rovira-Navarro:

Email: m.roviranavarro@tudelft.nl

Google Scholar (https://scholar.google.com/citations?hl=en&user=M0PCYCgAAAAJ) - Twitter (https://twitter.com/mroviranavarro)

Tiago Pestana:

Email: t.pestana@tudelft.nl

Google Scholar (https://scholar.google.com/citations?user=O-ch6P8AAAAJ&hl=en&oi=ao)

ABSTRACT

Saturn's moon Enceladus harbours a global subsurface ocean beneath its icy crust. Tidal dissipation within the moon's core generates a substantial amount of heat which leads to ocean convection. Understanding this transport of mass and heat within the ocean is key to understand exchange processes between core, ocean and ice shell. Previous studies of ocean convection assume oceans of constant thickness and constant superadiabatic temperature gradients between the inner core and outer ice shell. However, observations indicate ocean thickness variations of up to ~20 km from equator to pole and heterogenous tidal dissipation within the core likely results in latitude-dependent temperature gradients. In this study, we analyse how heterogeneities affect circulation patterns and heat transfer in an Enceladan ocean using three-dimensional direct numerical simulations. We focus on a degree-2 meridional thickness profile with varying degree of thermal forcing to analyse the different rotating convection regimes and compare them with those of an ocean of constant thickness. Our results show that the non-uniform ocean gives rise to a latitudinally variable Rayleigh number, causing a potential decoupling of rotating convection regimes experienced locally within the ocean. As in the constant ocean thickness scenario, different regimes of convection exist, which depend on the relative influence of rotation. With increasing thermal forcing, convection moves from being restricted to equatorial regions to filling the whole fluid domain. Heat transport efficiency, as measured by the local Nusselt number, is different for the uniform and non-uniform cases and depends on the convection regime. Nusselt-Rayleigh relations are similar to those obtained for an ocean of uniform thickness, but the relevant Rayleigh number depends on the region of the domain that is convecting.

REFERENCES

Čadek, O., Souček, O., Běhounková, M., Choblet, G., Tobie, G., & Hron, J. (2019). Long-term stability of Enceladus' uneven ice shell. Icarus, 319, 476-484.

Choblet, G., Tobie, G., Sotin, C., Běhounková, M., Čadek, O., Postberg, F., & Souček, O. (2017). Powering prolonged hydrothermal activity inside Enceladus. Nature Astronomy, 1(12), 841-847.

Gastine, T., Wicht, J., & Aubert, J. (2016). Scaling regimes in spherical shell rotating convection. Journal of Fluid Mechanics, 808, 690-732.

Hemingway, D. J., & Mittal, T. (2019). Enceladus's ice shell structure as a window on internal heat production. Icarus, 332, 111-131.

Liao, Y., Nimmo, F., & Neufeld, J. A. (2020). Heat production and tidally driven fluid flow in the permeable core of Enceladus. Journal of Geophysical Research: Planets, 125(9), e2019JE006209.

Soderlund, K. M. (2019). Ocean dynamics of outer solar system satellites. Geophysical Research Letters, 46(15), 8700-8710.